
Dynamic Dual Buffer with Divide-and-Conquer Strategy for Online Continual Learning

Congren Dai

Department of Computing
Imperial College London
United Kingdom

congren.dai@imperial.ac.uk

Huichi Zhou

Department of Bioengineering
Imperial College London
United Kingdom

h.zhou24@imperial.ac.uk

Jiahao Huang

Department of Bioengineering
Imperial College London
United Kingdom

j.huang21@imperial.ac.uk

Zhenxuan Zhang

Department of Bioengineering
Imperial College London
United Kingdom

z.zhenxuan24@imperial.ac.uk

Fanwen Wang

Department of Bioengineering
Imperial College London
United Kingdom

fanwen.wang@imperial.ac.uk

Guang Yang

Department of Bioengineering
Imperial College London
United Kingdom

g.yang@imperial.ac.uk

Fei Ye[†]

School of Information and Software Engineering
University of Electronic Science and Technology of China
China
fy689@uestc.edu.cn

Abstract

Online Continual Learning (OCL) presents a complex learning environment in which new data arrives in a batch-to-batch online format, and the risk of catastrophic forgetting can significantly impair model efficacy. In this study, we address OCL by introducing an innovative memory framework that incorporates a short-term memory system to retain dynamic information and a long-term memory system to archive enduring knowledge. Specifically, the long-term memory system comprises a collection of sub-memory buffers, each linked to a cluster prototype and designed to retain data samples from distinct categories. We propose a novel K -means-based sample selection method to identify cluster prototypes for each encountered category. To safeguard essential and critical samples, we introduce a novel memory optimisation strategy that selectively retains samples in the appropriate sub-memory buffer by evaluating each cluster prototype against incoming samples through an optimal transportation mechanism. This approach specifically promotes each sub-memory buffer to retain data samples that exhibit significant discrepancies from the corresponding cluster prototype, thereby ensuring the preservation of semantically rich information. In addition, we propose a novel Divide-and-Conquer (DAC) approach that formulates the memory updating as an optimisation problem and divides it into several subproblems. As a result, the proposed DAC approach can solve these subproblems separately and thus can significantly reduce computations of the proposed memory updating process. We conduct a series of experiments across standard and imbalanced learning settings, and the empirical findings indicate that the proposed memory framework achieves state-of-the-art performance in both learning contexts.

[†]Corresponding author.

1 Introduction

Humans and animals exhibit the remarkable ability to acquire new knowledge continuously from their environments while retaining previously learned information. This capability, known as Continual Learning (CL) [31], has emerged as a prominent research area within the field of deep learning. In contrast to traditional deep learning paradigms [15], which involve retraining on entire datasets multiple times, CL focuses on developing models that can sustain high performance across all prior tasks while assimilating new information. Nevertheless, contemporary learning models often experience considerable performance degradation in CL scenarios, primarily due to the phenomenon known as catastrophic forgetting [31].

The challenge of catastrophic forgetting arises when a model, while learning new tasks, gradually overwrites previously acquired knowledge. To mitigate this, existing work generally falls into three categories: rehearsal methods that store a small set of past examples in a memory buffer and replay them during training; regularisation methods that add penalty terms to the loss function to prevent drastic changes in important parameters; and architecture-based methods that expand the network by adding new layers for each incoming task. However, most rehearsal approaches rely on a single memory buffer, which struggles to balance the retention of both recent and distant experiences under limited capacity, leaving the model vulnerable to forgetting.

Additionally, another major challenge in CL is that most existing methodologies typically assume a static learning setting in which all past data can be revisited repeatedly and each class or task is perfectly balanced. These assumptions are rarely met in real-world scenarios. This focus overlooks a more complex and realistic CL context, characterised by the condition that each data batch is encountered only once, which we refer to as Online Continual Batch-to-Batch Learning (OCBBL). In this paper, we endeavour to tackle catastrophic forgetting under both the OCBBL and the dataset imbalance settings by introducing an innovative memory-based strategy.

Biological findings indicate that in human learning systems, knowledge is continuously processed in the brain through both fast and slow memory mechanisms [30]. Drawing inspiration from the findings, we propose Online Dynamic Expandable Dual Memory (ODEDM), which integrates a lightweight short-term buffer for transient inputs and a prototype-based long-term memory split into per-task sub-buffers. New samples first enter the short-term buffer to minimise overhead, while the long-term memory is organised by K -means [28] into cluster prototypes, each spawning an expandable sub-buffer that holds a fixed, balanced number of semantically similar samples per category. To decide which incoming samples augment a prototype’s sub-buffer, we compute the Optimal Transport (OT) distance between each sample and its nearest prototype, ensuring semantic similarity to represent the whole data. During training, we dynamically allocate capacity: initially expanding the short-term buffer to accelerate convergence, then progressively shifting slots to long-term sub-buffers to mitigate forgetting. Finally, a recursive divide-and-conquer clustering scheme groups samples hierarchically around prototypes, dramatically reducing the computational cost of maintaining and updating the memory system.

We conduct a series of experiments on both standard and imbalanced settings to evaluate the performance of various models and the empirical results demonstrate that the proposed approach achieves state-of-the-art performance in various CL scenarios. The contributions of this paper are summarised into three parts : (1) Inspired by the biological findings, we propose a novel training framework that incorporates short- and long-term memory buffers with dynamically changing sizes to address catastrophic forgetting in the OCBBL scenario; (2) This plug-and-play framework is designed to be compatible with rehearsal-based models, and it is shown experimentally to enhance their performance. (3) We also propose a novel DAC approach that divides a more complex problem into several subproblems and solves them separately. The proposed DAC approach can significantly reduce the computational cost of ODEDM.

2 Related work

Rehearsal-based approaches aim to replay old data to prevent forgetting and can be divided into three categories: experience replay, generative replay, and feature replay [39]. The experience replay typically utilises a memory buffer to store old training data and replay them during the new task learning, such as reservoir sampling [7, 33, 38] that selectively retains a constant number of previously acquired training samples from each batch in a stochastic manner. Dark Experience Replay (DER)

and DER++ [4] retain previous training samples as well as their corresponding logits, and design a loss function to improve the model’s generalisation performance in CL. The generative replay, which often involves training an auxiliary generative model to replay synthesised data, has shown significant performance in CL. Deep Generative Replay (DGR) [36] learns each new task that is accompanied by replaying data generated by the previous model, enabling the retention of prior knowledge. Memory Replay GANs (MeRGAN) [42] employs a Generative Adversarial Net (GAN) as a generative replay network that can continually produce old samples to relieve network forgetting. Lastly, the feature replay method aims to train a generative model to learn the feature information. During the new task learning, old feature vectors are drawn from the generative replay network to relieve network forgetting. Such an approach is proposed in recent studies, including Generative Feature Replay (GFR) [27], Feature Adaptation (FA) [19], and Dynamic Structure Reorganisation (DSR) [47].

Regularisation-based techniques can be divided into two main categories: weight-based and function-based, depending on their regularisation objectives [39]. Weight regularisation approaches focus on mitigating catastrophic forgetting by imposing penalties on alterations in the network weights. A prominent example of this category is Elastic Weight Consolidation (EWC) [22], which assesses the significance of each parameter within the network and penalises modifications to those critical parameters. Conversely, function regularisation methods utilise knowledge distillation (KD) [13] to address catastrophic forgetting. In these approaches, the model trained on the previous task serves as a teacher module, while the current model acts as a student module. The objective is to minimise the distance between the outputs of the teacher and student when processing samples from a new task, thereby alleviating the issue of network forgetting [11, 19, 26, 6, 12, 17, 42, 46].

Architecture-based approaches focus on acquiring a set of parameters applicable to all previously learned tasks. Specifically, upon the completion of learning the current task, these methods preserve prior knowledge by freezing all previously acquired parameters and subsequently generating a new sub-model tailored for the new task [39]. Prior studies generally categorise architecture-based methods into two main types: parameter isolation and dynamic expansion. Parameter isolation techniques, such as Piggyback [29], Supermasks in Superposition (SupSup) [41], and Winning Subnetworks (WSN) [21], focus on training a single network where only a limited portion of the parameter set is modified to accommodate the new task, while the remaining parameters remain unchanged. Conversely, dynamic expansion methods, including Dynamically Expandable Networks (DEN) [44] and Compacting, Picking and Growing (CPG) [18], are designed to incrementally introduce new hidden layers and nodes to effectively address the learning requirements of a new task.

3 Methodology

3.1 Problem Formulation

The traditional CL setting considers that the model can revisit the task-specific training dataset multiple times, which can not be applied to an online batch-to-batch manner. In this paper, we focus on this challenging CL scenario where each sample is only seen once during the training. Let $T = \{T_1, T_2, \dots, T_n\}$ denote a series of n tasks, and each task T_i contains a training dataset $D_i = \{\mathbf{x}_j, \mathbf{y}_j\}_{j=1}^{n_i}$, where \mathbf{x}_j and \mathbf{y}_j represent the sample and the associated label over the data space $\mathcal{X} \in \mathbb{R}^d$ and the label space $\mathcal{Y} \in \mathbb{R}^{d_y}$, in the given order. d and d_y denote the dimension of the data and label space, respectively. n_i is the total number of data samples from D_i . In a class-incremental learning scenario, we can create a data stream S by combining these datasets, expressed as :

$$S = \{D_1, \dots, D_n\}. \quad (1)$$

Under the OCBBL setting, the data stream S is divided into n' data batches $\{(\mathbf{X}_1, \mathbf{Y}_1), \dots, (\mathbf{X}_{n'}, \mathbf{Y}_{n'})\}$, where each data batch consists of b number of samples. At a certain training time t_i (the i -th training time), we can only obtain the associated data batch $(\mathbf{X}_i, \mathbf{Y}_i)$ and can not access all previous data batches $\{(\mathbf{X}_1, \mathbf{Y}_1), \dots, (\mathbf{X}_{i-1}, \mathbf{Y}_{i-1})\}$. A model updated at the i -th training time is to minimise the loss across all data batches, expressed as :

$$\theta^* = \operatorname{argmin}_{\theta \in \Theta} \sum_{j=1}^i \sum_{c=1}^{|\mathbf{X}_j|} \mathcal{L}_{\text{CE}}(\mathbf{y}_{(c,j)}, f_\theta(\mathbf{x}_{(c,j)})), \quad (2)$$

where Θ represents parameter space and θ^* is the optimal parameter set that minimises the loss on all previously seen data batches $\{(\mathbf{X}_1, \mathbf{Y}_1), \dots, (\mathbf{X}_{n'}, \mathbf{Y}_{n'})\}$. $\mathbf{x}_{(c,j)}$ and $\mathbf{y}_{(c,j)}$ denote the c -th labelled sample from the j -th data batch $(\mathbf{X}_j, \mathbf{Y}_j)$. However, optimising Equation (2) is intractable

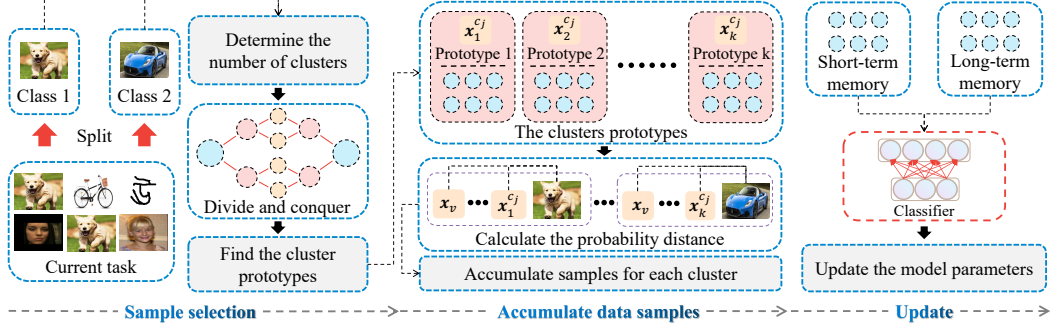


Figure 1: The optimisation procedure for the proposed ODEDM approach consists of three steps. In the first step, we determine several memory clusters using the K -means algorithm. The second step uses the divide-and-conquer method to refine the clusters, and then selectively stores diverse samples into the appropriate memory cluster. In the third step, we employ all memorised samples and the incoming data batch to update the model.

in online CL because we can not utilise all previous data batches. To solve this issue, this paper aims to develop a novel memory approach that stores a few past critical samples to minimise the loss defined in Equation (2). Once the whole training process is finished, we evaluate the model’s performance on all testing samples.

3.2 The Memory Structure

The proposed ODEDM approach consists of a short-term memory system $\mathcal{M}_i^{\text{short}}$ and a long-term memory system $\mathcal{M}_i^{\text{long}}$ to preserve both temporary and permanent information, respectively, where the subscript i denotes the memory buffer updated at the i -th task learning. For the short-term memory buffer, we adopt the reservoir sampling to randomly choose and store new data samples, which is computationally efficient.

For the long-term memory buffer, we aim to preserve more critical and diverse data samples across all previously learned categories. In order to ensure balanced samples in the memory buffer, we propose to define several memory prototypes per category, while each prototype aims to accumulate similar data samples and form a sub-memory buffer. Let c_j denote the j -th category and $\mathbf{x}_h^{c_j}$ represent the h -th cluster prototype for the category c_j . Let $\mathcal{M}(c_j, h)$ denote the sub-memory buffer formed using the cluster prototype $\mathbf{x}_h^{c_j}$. Each sub-memory buffer $\mathcal{M}(c_j, h)$ has a maximum memory size, denoted by λ .

The sample selection. In order to ensure balanced samples in the memory system, we introduce a novel sample selection approach that determines an equal number of cluster prototypes for each category. Specifically, for a given new task T_i , we first calculate a number of cluster prototypes required for the category c_j using the function $F_k(\rho)$, expressed as :

$$F_k(\rho) = \left[\frac{\rho \lambda_{\max}}{n-1} \cdot \frac{1}{|\mathbf{C}^i|} \right], \quad (3)$$

where \mathbf{C}^i denotes a set of all categories for T_i and $|\mathbf{C}^i|$ represents the total number of categories. ρ is a hyperparameter used as the proportion of the long-term memory buffer in the whole memory system. Specifically, we employ the K -means algorithm $F_{\text{centre}}(D_i(c_j), c_j)$ to determine the cluster prototypes $\{\mathbf{x}_1^{c_j}, \dots, \mathbf{x}_k^{c_j}\}$ for the category c_j from the dataset of the i -th task learning, where $k = F_k(\rho)$ and $D_i(c_j)$ denotes the data samples from the j -th category.

3.3 Memory Optimisation Via Sinkhorn Distance

To encourage each memory prototype to accumulate more appropriate data samples into the associated sub-memory buffer, we propose to employ a probability distance to evaluate the knowledge similarity between each sub-memory buffer and candidate samples. Specifically, we consider employing the Wasserstein distance [37], which is a popular probability measure. The main idea of the Wasserstein distance is to quantify the minimum cost of a probability measure \mathbb{A} into another probability

measure \mathbb{B} , aiming to solve OT Problems [35]. Let (M, π) be the metric space, where $\pi(\mathbf{x}^1, \mathbf{x}^2)$ represents the distance between \mathbf{x}^1 and \mathbf{x}^2 in the set M . The p -th Wasserstein distance is defined as :

$$W_p(\mathbb{A}, \mathbb{B}) = \left(\inf_{\mu \in \Gamma(\mathbb{A}, \mathbb{B})} \int \rho(\mathbf{x}^1, \mathbf{x}^2)^p d\mu(\mathbf{x}^1, \mathbf{x}^2) \right)^{1/p}, \quad (4)$$

where $\Gamma(\mathbb{A}, \mathbb{B})$ is the set of all joint distributions $\mu(\mathbf{x}^1, \mathbf{x}^2)$ on $M \times M$ with marginals $\mathbb{A}, \mathbb{B} \in \{\mathbb{A} : \int \pi(\mathbf{x}^1, \mathbf{x}^2)^p d\mathbb{B}(\mathbf{x}^1) < \infty, \forall y \in M\}$.

One of the primary weaknesses of using the Wasserstein distance is its considerable computational costs, which is not suitable when considering using it in our approach. To address this issue, we consider employing the Sinkhorn distance [9], which is one of the OT measures. Specifically, the Sinkhorn distance introduces a smoothing term to transform the optimisation into a strictly convex problem. As a result, this problem can be solved using Sinkhorn's matrix scaling algorithm, which converges rapidly through iterative matrix-vector multiplications, which is computationally efficient. According to [9], we can define the Sinkhorn distance as :

$$f_\alpha(\mathbf{a}, \mathbf{b}) := \min_{P \in U_\alpha(\mathbf{a}, \mathbf{b})} \langle P, M \rangle, \quad (5)$$

where $U_\alpha(\mathbf{a}, \mathbf{b})$ is the convex set, expressed as :

$$\begin{aligned} U_\alpha(\mathbf{a}, \mathbf{b}) &:= \{P \in U(\mathbf{a}, \mathbf{b}) \mid D_{KL}(P \parallel \mathbf{a}\mathbf{b}^T) \leq \alpha\} \\ &= \{P \in U(\mathbf{a}, \mathbf{b}) \mid h'(P) \geq h'(\mathbf{a}) + h'(\mathbf{b}) - \alpha\} \subset U(\mathbf{a}, \mathbf{b}), \end{aligned}$$

where $D_{KL}(P \parallel \mathbf{a}\mathbf{b}^T) = h'(\mathbf{b}) + h'(\mathbf{a}) - h'(P)$ represents the Kullback-Leibler (KL) divergence [25]. $U(\mathbf{a}, \mathbf{b})$ is the transport polytope of \mathbf{b} and \mathbf{a} , expressed as $U(\mathbf{a}, \mathbf{b}) := \{P \in \mathbb{R}_+^{d \times d}, P\mathbf{I}_d = \mathbf{a}, P^T\mathbf{I}_d = \mathbf{b}\}$. \mathbf{a} and \mathbf{b} are two probability vectors and $h'(\cdot)$ is the entropy function. P is a joint probability and M is a cost matrix mapping of \mathbf{a} to \mathbf{b} . The superscript T denotes the transposition of a matrix. We calculate the distance $f_\alpha(\cdot, \cdot)$ using the matrix scaling algorithm [8], which receives a pair of data samples. Compared to the Wasserstein distance, the Sinkhorn distance has a faster computing speed and can be evaluated on high-dimensional spaces. Based on Equation (5), we can employ f_α to choose appropriate samples for each sub-memory buffer.

For a given new task T_j , we determine the cluster prototypes $\{\mathbf{x}_1^{c_j}, \dots, \mathbf{x}_k^{c_j}\}$ using the proposed sample selection approach. Then we propose a novel Sinkhorn distance-based sample selection approach to accumulate samples for each memory centre $\mathbf{x}_h^{c_j}, h = 1, \dots, k$, expressed as :

$$\mathcal{M}(c_j, h) = \{\mathbf{x}_v \mid \mathbf{x}_v \in D_i(c_j), v = 1, \dots, \lambda - 1, f_\alpha(\mathbf{x}_v, \mathbf{x}_h^{c_j}) > f_\alpha(\mathbf{x}_{v+1}, \mathbf{x}_h^{c_j})\}, \quad (6)$$

where $D_i(c_j)$ is the subset consisting of samples of the category c_j obtained using the function $F_{\text{class}}(\cdot)$, expressed as :

$$F_{\text{class}}(D_i, c_j) = \{\mathbf{x}_v \mid \mathbf{x}_v \in D_i, v = 1, \dots, |D_i|, f_{\text{true}}(\mathbf{x}_v) = c_j\}, \quad (7)$$

where $f_{\text{true}}(\cdot)$ is the function that always returns the true label for the given input \mathbf{x}_v . Specifically, we employ $f_\alpha(\cdot)$ to calculate a pair of samples in order to reduce computational costs. Equation (6) aims to choose the data samples that are closest to the cluster prototypes, which can help preserve statistically representative information for c_j .

3.4 Dynamic Memory Allocation

As the number of tasks, employing the fixed capacity for the short-term memory buffer would not preserve sufficient training samples for the model at the initial training stage. In this paper, we address this issue by introducing a novel dynamic memory allocation approach that dynamically allocates samples in short- and long-term memory buffers. As a result, the short-term memory can store sufficient training samples at the initial learning phase and gradually transfers its capacities to the long-term memory buffer as the number of tasks increases. Let λ_{max} denote the maximum memory size for the proposed memory approach. At the first task learning, the short-term memory buffer can use the full memory capacity (the maximum memory size is λ_{max}) to store data samples while the long-term memory buffer is empty. In the second task learning, we have a default hyperparameter k , which is used to denote the number of cluster prototypes per category. Then we find the cluster

prototypes and use each one of them to store critical data samples into the associated sub-memory buffer.

Once the i -th task learning is finished, we propose to employ Equation (6) to find a set of sub-memory buffers $\{\mathcal{M}(c_j, 1), \dots, \mathcal{M}(c_j, k)\}$ using Equation (6). Then, the long-term memory buffer is updated by :

$$\mathcal{M}_j^{\text{long}} = \hat{\mathcal{M}}_j^{\text{long}} \bigcup \mathcal{M}(c_j, 1) \dots \bigcup \mathcal{M}(c_j, k), \quad (8)$$

where $\hat{\mathcal{M}}_j^{\text{long}}$ denotes the long-term memory buffer before the updating process. As a result, we randomly remove data samples of the short-term memory buffer $\mathcal{M}_j^{\text{short}}$ until the total number of memorised samples is equal to the maximum memory size. This dynamic memory allocation strategy facilitates the progressive expansion of the long-term memory buffer while correspondingly reducing the short-term memory buffer, thereby enhancing the retention of critical historical samples over time.

3.5 Memory Optimisation Algorithm

In this section, we provide the detailed optimisation procedure of the proposed ODEDM approach in Figure 1, and we provide the pseudocode of the proposed ODEDM approach in **Algorithm 1** from the Supplementary Material (SM) in Appendix-A, respectively. The algorithmic description of the proposed ODEDM consists of three steps :

Step 1 (Find the cluster prototype). When seeing a new task T_i , we first calculate the number of memory clusters per category using the function defined by Equation (3).

Step 2 (Accumulate the data samples). For each memory cluster, we employ Equation (6) to selectively store appropriate data samples. These sub-memory buffers are added to the long-term memory buffer. Also, we update the short-term memory buffer using the reservoir sampling.

Step 3 (Update the model). We replay samples from both short- and long-term memory buffers to update the model using the cross-entropy loss function.

A computational defect is observed in ODEDM, which takes a significant runtime for a buffer size of 5120. Therefore, we also propose a method called Divide-and-Conquer (DAC) to mitigate this issue. The DAC method is designed to recursively merge point clouds until it reaches the k required for ODEDM to train properly. This is particularly useful for large datasets where direct computation of pairwise distances can be computationally expensive. As shown in **Algorithm 2** from the SM in Appendix-A, the DAC method operates as follows:

Step 1 (Initial partition). Split the input point set into K clusters via the K -Means algorithm, yielding $\{\mathcal{C}_1, \dots, \mathcal{C}_K\}$. It is noted that the K for DAC is different from the k for ODEDM.

Step 2 (Build point clouds). Convert each cluster \mathcal{C}_i into a tensor \mathcal{P}_i .

Step 3 (Pairwise distances). Compute the full symmetric distance matrix $D \in \mathbb{R}^{K \times K}$ by applying the Sinkhorn approximation of the Wasserstein distance to every pair $(\mathcal{P}_i, \mathcal{P}_j)$.

Step 4 (Select merge path). Enumerate all combinations of two or more clouds whose total size meets or exceeds the minimum constraint m (it should be larger than the k_i in **Algorithm 1** to make it function properly), and choose the path π^* with the smallest cumulative distance $\sum_t D_{\pi_t^*, \pi_{t+1}^*}$.

Step 5 (Merge and recurse). The selected point clouds, denoted as $\bigcup_{i \in \pi^*} \mathcal{P}_i$, are concatenated into a single aggregated set. Subsequently, the recursion depth is decremented, and the DAC procedure is recursively invoked on this merged point cloud. Recursion terminates when either no valid merge path exists (i.e., $\pi^* = \emptyset$) or the depth limit is reached, at which point the current cloud is returned as the final cluster, constrained by the number of k in ODEDM.

4 Experiments

4.1 Experiment Settings

Specifically, we consider many standard CL datasets and split each dataset into several tasks, and then we split CIFAR10 [23] and TINYIMG [43] into 5 and 10 tasks according to [10, 45], each of which contains 2 and 20 classes, in the stated order. We also follow [40] to split CIFAR100 [24] into 10 tasks, each of which contains samples from ten classes. In addition, we also consider a more challenging setting, called the imbalanced learning setting where it takes out the samples indexed by

Table 1: Comparison of standard vs. imbalanced settings, averaged over three runs.

Buffer	Method	CIFAR10				CIFAR100				TINYIMG			
		Standard		Imbalanced		Standard		Imbalanced		Standard		Imbalanced	
		Class-IL	Task-IL	Class-IL	Task-IL	Class-IL	Task-IL	Class-IL	Task-IL	Class-IL	Task-IL	Class-IL	Task-IL
200	DER [4]	21.29 _{±0.64}	81.25 _{±0.19}	18.69 _{±0.88}	73.61 _{±0.02}	04.40 _{±0.98}	34.00 _{±0.67}	04.01 _{±0.23}	30.37 _{±0.87}	04.33 _{±0.06}	27.15 _{±0.47}	04.02 _{±0.56}	20.86 _{±0.75}
	DER w/ ODEDM	29.99 _{±0.48}	69.61 _{±0.76}	22.04 _{±0.85}	67.07 _{±0.62}	04.78 _{±0.56}	25.53 _{±0.25}	03.20 _{±0.71}	20.77 _{±0.63}	03.83 _{±0.27}	17.21 _{±0.29}	02.82 _{±0.45}	14.44 _{±0.40}
	DER++ [4]	29.67 _{±0.20}	82.60 _{±0.49}	28.74 _{±0.10}	82.80 _{±0.16}	05.73 _{±0.24}	41.51 _{±0.26}	05.99 _{±0.48}	36.52 _{±0.08}	04.97 _{±0.63}	31.25 _{±0.20}	04.43 _{±0.85}	25.56 _{±0.28}
	DER++ w/ ODEDM	42.71 _{±0.86}	79.53 _{±0.49}	40.95 _{±0.82}	82.27 _{±0.05}	07.78 _{±0.78}	38.21 _{±0.48}	07.46 _{±0.17}	38.66 _{±0.79}	04.65 _{±0.16}	27.17 _{±0.65}	04.09 _{±0.95}	26.70 _{±0.11}
	DER++refresh [40]	31.91 _{±0.48}	86.49 _{±0.33}	30.24 _{±0.87}	74.38 _{±0.60}	05.04 _{±0.64}	41.26 _{±0.79}	05.43 _{±0.18}	40.30 _{±0.94}	05.74 _{±0.53}	34.15 _{±0.96}	04.28 _{±0.68}	27.10 _{±0.53}
	DER++refresh w/ ODEDM	42.47 _{±0.08}	85.56 _{±0.74}	38.41 _{±0.88}	79.79 _{±0.75}	08.47 _{±0.24}	41.17 _{±0.88}	05.68 _{±0.11}	34.87 _{±0.62}	05.25 _{±0.09}	28.04 _{±0.88}	03.29 _{±0.73}	23.28 _{±0.68}
	FDR [1]	20.31 _{±0.38}	69.93 _{±0.02}	14.75 _{±0.85}	69.37 _{±0.89}	06.09 _{±0.98}	34.71 _{±0.53}	04.25 _{±0.97}	27.84 _{±0.44}	04.55 _{±0.57}	25.32 _{±0.31}	03.55 _{±0.17}	19.50 _{±0.77}
	FDR w/ ODEDM	25.17 _{±0.39}	73.76 _{±0.58}	21.14 _{±0.72}	68.20 _{±0.27}	04.14 _{±0.52}	23.10 _{±0.18}	05.49 _{±0.55}	21.11 _{±0.55}	04.18 _{±0.31}	18.65 _{±0.00}	03.51 _{±0.50}	15.70 _{±0.60}
	iCaRL [32]	35.32 _{±0.28}	88.99 _{±0.05}	34.39 _{±0.53}	84.85 _{±0.48}	08.56 _{±0.37}	35.59 _{±0.58}	07.41 _{±0.30}	33.79 _{±0.61}	03.78 _{±0.19}	19.16 _{±0.52}	03.61 _{±0.05}	17.82 _{±0.48}
	iCaRL w/ ODEDM	37.64 _{±0.16}	89.88 _{±0.72}	35.26 _{±0.08}	81.94 _{±0.76}	01.03 _{±0.02}	07.05 _{±0.19}	01.17 _{±0.04}	06.28 _{±0.33}	—	—	—	—
500	DER [4]	20.56 _{±0.26}	85.74 _{±0.29}	17.25 _{±0.49}	82.62 _{±0.78}	04.49 _{±0.21}	33.45 _{±0.38}	03.89 _{±0.60}	30.81 _{±0.40}	04.21 _{±0.48}	26.34 _{±0.34}	03.17 _{±0.11}	22.07 _{±0.13}
	DER w/ ODEDM	28.34 _{±0.14}	70.96 _{±0.37}	21.32 _{±0.05}	62.80 _{±0.85}	04.12 _{±0.81}	24.88 _{±0.12}	03.84 _{±0.08}	23.59 _{±0.54}	04.45 _{±0.12}	20.52 _{±0.06}	03.55 _{±0.17}	18.28 _{±0.57}
	DER++ [4]	39.85 _{±0.20}	86.08 _{±0.48}	32.94 _{±0.58}	82.21 _{±0.42}	08.42 _{±0.01}	49.41 _{±0.29}	05.27 _{±0.54}	41.87 _{±0.81}	06.72 _{±0.01}	39.53 _{±0.22}	05.44 _{±0.00}	33.92 _{±0.55}
	DER++ w/ ODEDM	47.31 _{±0.62}	83.46 _{±0.10}	40.14 _{±0.46}	82.85 _{±0.65}	13.62 _{±0.25}	50.26 _{±0.28}	10.16 _{±0.55}	44.82 _{±0.34}	07.43 _{±0.75}	34.96 _{±0.37}	05.93 _{±0.12}	32.56 _{±0.17}
	DER++refresh [40]	43.58 _{±0.29}	85.71 _{±0.02}	29.73 _{±0.82}	82.31 _{±0.58}	09.99 _{±0.70}	36.13 _{±0.85}	07.56 _{±0.98}	45.27 _{±0.73}	06.86 _{±0.88}	39.53 _{±0.38}	05.92 _{±0.03}	32.95 _{±0.99}
	DER++refresh w/ ODEDM	46.17 _{±0.27}	85.56 _{±0.28}	41.53 _{±0.15}	77.49 _{±0.91}	11.79 _{±0.91}	47.21 _{±0.63}	10.27 _{±0.19}	07.14 _{±0.85}	35.66 _{±0.90}	07.00 _{±0.79}	33.13 _{±0.75}	—
	FDR [1]	18.23 _{±0.43}	68.27 _{±0.40}	17.96 _{±0.28}	73.70 _{±0.25}	04.80 _{±0.69}	32.71 _{±0.47}	03.49 _{±0.38}	27.94 _{±0.77}	04.22 _{±0.10}	22.54 _{±0.97}	04.17 _{±0.00}	19.15 _{±0.85}
	FDR w/ ODEDM	24.43 _{±0.27}	76.23 _{±0.24}	17.50 _{±0.57}	59.64 _{±0.36}	04.96 _{±0.84}	04.71 _{±0.66}	28.67 _{±0.96}	33.81 _{±0.27}	04.84 _{±0.38}	21.14 _{±0.48}	03.90 _{±0.27}	17.04 _{±0.90}
	iCaRL [32]	35.16 _{±0.17}	84.89 _{±0.51}	32.74 _{±0.74}	87.46 _{±0.57}	09.04 _{±0.54}	36.81 _{±0.94}	08.25 _{±0.55}	34.53 _{±0.55}	04.19 _{±0.24}	20.09 _{±0.56}	03.89 _{±0.12}	18.59 _{±0.00}
	iCaRL w/ ODEDM	38.31 _{±0.12}	86.81 _{±0.33}	36.10 _{±0.87}	85.30 _{±0.96}	07.35 _{±0.14}	07.49 _{±0.20}	05.21 _{±0.27}	33.70 _{±0.27}	04.48 _{±0.08}	03.59 _{±0.14}	00.51 _{±0.02}	03.62 _{±0.39}
5120	DER [4]	24.65 _{±0.26}	84.07 _{±0.55}	17.38 _{±0.60}	74.88 _{±0.59}	04.26 _{±0.23}	31.26 _{±0.21}	04.43 _{±0.31}	31.32 _{±0.32}	04.30 _{±0.26}	30.55 _{±0.65}	03.81 _{±0.28}	26.81 _{±0.97}
	DER w/ ODEDM	29.96 _{±0.13}	66.24 _{±0.21}	21.89 _{±0.60}	63.16 _{±0.46}	04.83 _{±0.33}	26.29 _{±0.48}	02.92 _{±0.78}	18.88 _{±0.64}	04.49 _{±0.48}	20.28 _{±0.52}	03.55 _{±0.37}	18.27 _{±0.50}
	DER++ [4]	43.31 _{±0.12}	86.26 _{±0.14}	39.16 _{±0.28}	83.81 _{±0.33}	11.98 _{±0.84}	57.62 _{±0.57}	07.89 _{±0.34}	46.23 _{±0.71}	09.06 _{±0.80}	51.00 _{±0.69}	08.05 _{±0.07}	46.06 _{±0.18}
	DER++ w/ ODEDM	54.49 _{±0.14}	87.77 _{±0.22}	47.90 _{±0.10}	87.37 _{±0.42}	22.42 _{±0.67}	61.76 _{±0.50}	13.62 _{±0.94}	53.41 _{±0.23}	15.61 _{±0.29}	51.29 _{±0.23}	11.13 _{±0.12}	45.89 _{±0.38}
	DER++refresh [40]	47.78 _{±0.63}	88.64 _{±0.29}	34.19 _{±0.74}	81.72 _{±0.88}	08.33 _{±0.01}	53.64 _{±0.20}	05.81 _{±0.90}	39.67 _{±0.60}	10.21 _{±0.49}	50.38 _{±0.32}	07.34 _{±0.24}	43.39 _{±0.99}
	DER++refresh w/ ODEDM	55.17 _{±0.20}	80.32 _{±0.62}	45.22 _{±0.04}	84.50 _{±0.13}	21.60 _{±0.37}	63.24 _{±0.88}	15.15 _{±0.02}	52.73 _{±0.98}	17.65 _{±0.43}	53.27 _{±0.02}	12.71 _{±0.17}	47.61 _{±0.07}
	FDR [1]	19.33 _{±0.17}	79.53 _{±0.26}	13.47 _{±0.04}	66.57 _{±0.28}	04.97 _{±0.75}	36.85 _{±0.76}	04.23 _{±0.41}	33.16 _{±0.56}	05.06 _{±0.38}	22.44 _{±0.29}	04.20 _{±0.63}	21.73 _{±0.64}
	FDR w/ ODEDM	18.33 _{±0.58}	64.53 _{±0.49}	17.86 _{±0.14}	61.47 _{±0.36}	06.04 _{±0.94}	29.69 _{±0.68}	04.94 _{±0.12}	28.15 _{±0.63}	05.01 _{±0.23}	23.18 _{±0.81}	04.69 _{±0.22}	20.94 _{±0.30}
	iCaRL [32]	47.12 _{±0.70}	86.20 _{±0.43}	34.48 _{±0.25}	82.29 _{±0.68}	09.46 _{±0.13}	37.47 _{±0.97}	08.41 _{±0.54}	34.45 _{±0.74}	04.09 _{±0.31}	20.45 _{±0.64}	03.97 _{±0.18}	19.17 _{±0.98}
	iCaRL w/ ODEDM	47.50 _{±0.88}	89.27 _{±0.56}	44.78 _{±0.21}	85.40 _{±0.81}	09.28 _{±0.14}	36.51 _{±0.64}	08.33 _{±0.16}	35.38 _{±0.44}	04.01 _{±0.02}	19.10 _{±0.19}	03.83 _{±0.18}	18.23 _{±0.47}

even numbers such as $\{0, 2, 4, \dots, n\} \in \text{class}$ for the proposed dual buffer and dynamic dual buffer methods, resulting IMB-CIFAR10, IMB-CIFAR100 and IMB-TINYIMG.

Baselines. In this paper, we consider to compare our method with the following baselines: DER [4], DER++ [4], DER++refresh [40], The False Discovery Rate (FDR) [1], Incremental Classifier and Representation Learning (iCaRL) [32]. DER leverages "dark knowledge" (logits) through knowledge distillation and replay of prior experiences selected via reservoir sampling, aiming to counter catastrophic forgetting without dependence on task demarcations. DER++ refines this approach by incorporating ground truth labels in addition to stored logits, thus boosting performance in CL. DER++refresh further refines the DER++ by implementing an "unlearn-relearn" mechanism, which strategically discards obsolete information to enhance generalisation and adaptability when assimilating new tasks.

DAC parameters. As DAC has two hyperparameters, K and $depth$, we set K from 3 to 5 and $depth$ from 2 to 4 for each proportion of long-term memory size. We run the hyperparameter experiments using the proposed ODEDM on the CIFAR10 and DER++refresh as the training model to compare the performance of DAC. The optimal hyperparameters corresponding to each proportion of long-term memory size are presented in Table 3 from the SM in Appendix-B. Accordingly, for buffer sizes of 200 and 500, we adopt ($K = 3$, $depth = 4$) for the 25% setting, ($K = 3$, $depth = 2$) for 50%, and ($K = 5$, $depth = 3$) for 75%. For a buffer size of 5120, we consistently apply ($K = 5$, $depth = 3$) across the 25%, 50%, and 75% settings to maintain computational efficiency.

Ablation. For the ablation study, we use DER++refresh as the baseline model, 200 as the buffer size, and CIFAR10 as the dataset under the standard setting. First, we consider the following settings for dynamic dual buffer : (1) Mixup; (2) ODEDM without DAC; (3) ODEDM with DAC. The Mixup method is a vanilla implementation for ODEDM to select the prototypes for the long-term memory buffer by averaging samples from each cluster. Additionally, we use L1, L2, Maximum Mean Discrepancy (MMD) [14], and Sinkhorn distances as the distance metric in ODEDM and DAC to compare differences. We use Radial Basis Function (RBF) kernel [3] for the MMD distance.

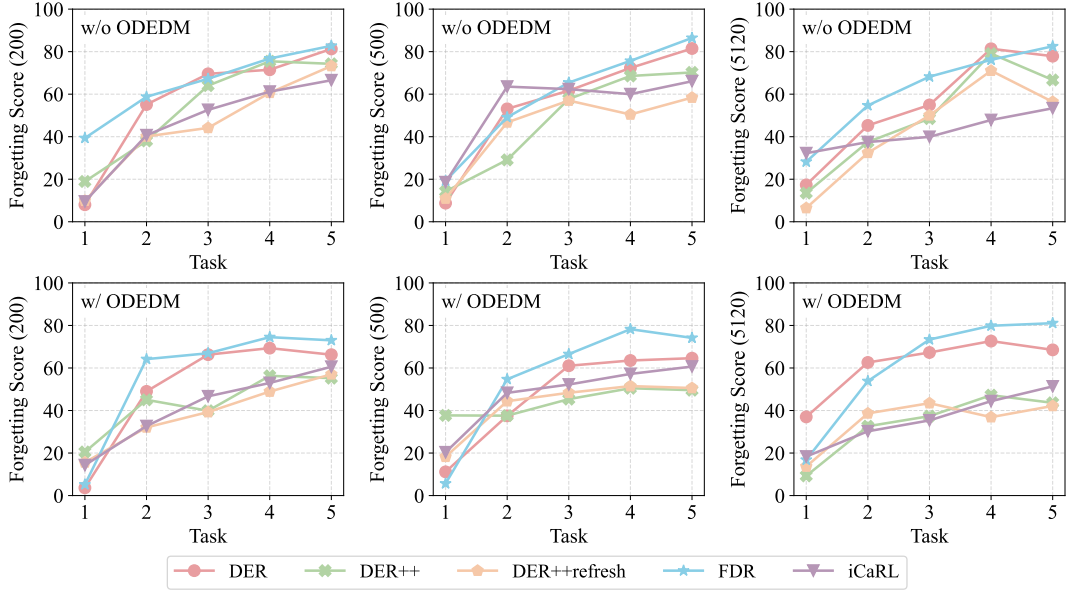


Figure 2: Forgetting curve analysis for the CIFAR10, achieved by various models trained using different memory configurations. The results show the forgetting scores (\downarrow) for buffer sizes of 200, 500, and 5120 under the standard setting.

4.2 Empirical Results

Standard setting. The Class-IL accuracy of models employing ODEDMD, as reported in Table 1, corresponds to the optimal accuracy presented in Tables 4 to 6 from the SM in Appendix-B, given different proportions of long-term memory size. Augmenting rehearsal methods with our proposed ODEDMD yields consistent and substantial improvements in Class-IL accuracy across all datasets and buffer sizes. For example, DER++ on CIFAR10 with a buffer of size 200 increases from 29.7% to 42.7% when using ODEDMD, and even at the largest buffer size of 5120, DER++ with ODEDMD raises Class-IL performance from 43.3% to 54.5%. Similar trends hold for CIFAR-100 and TINYIMG, where gains of 5-15 percentage points (pp) are observed. In contrast, Task-IL accuracy, which assumes known task identities, sees minimal change or slight decreases, reflecting that our model primarily enhances cross-task representation rather than within-task discrimination.

Different rehearsal variants respond differently to model integration. The relative gap between DER and DER++ widens when using the model: although DER++ already surpasses DER in its vanilla form, adding our model brings disproportionately larger gains to DER++. The refresh mechanism in DER++ refresh already captures some benefits that ODEDMD provides, so the incremental improvements there are meaningful but smaller. FDR, as a lightweight regularisation baseline, starts from lower absolute scores yet still gains 4-5 pp in Class-IL on CIFAR10 and CIFAR100 when augmented. In contrast, iCaRL demonstrates an unexpected performance collapse on CIFAR100 and fails to produce results on TINYIMG under the small-buffer regimes combined with ODEDMD. This degradation is likely attributable to conflicts between its nearest-mean classifier and the altered feature representations induced by ODEDMD, as well as limitations in its rehearsal mechanism, which struggles to accumulate sufficient samples. Nevertheless, performance recovers when larger buffer sizes are employed.

The impact of ODEDMD is most pronounced in memory-constrained regimes. With buffers of size 200 or 500, Class-IL accuracy on CIFAR10 jumps by 8-15 pp and up to 5 pp on CIFAR100, underscoring high value when rehearsal memory is limited. Yet even at a buffer size of 5120, the model continues to deliver double-digit gains (e.g., +11 pp on CIFAR10, +10 pp on CIFAR100), demonstrating scalability to larger memory budgets. Across all experiments, Task-IL results exceed Class-IL by 40-60 pp, reaffirming that known task identities simplify CL. Our ODEDMD excels at mitigating inter-task interference in Class-IL, rather than enhancing intra-task discrimination.

Imbalanced setting. In Table 1, under imbalanced class distributions, all methods suffer a performance drop relative to the standard setting, yet integrating our model markedly narrows this gap. On CIFAR10 with a buffer of 200, DER++ with ODEDMD maintains 40.9% Class-IL accuracy under

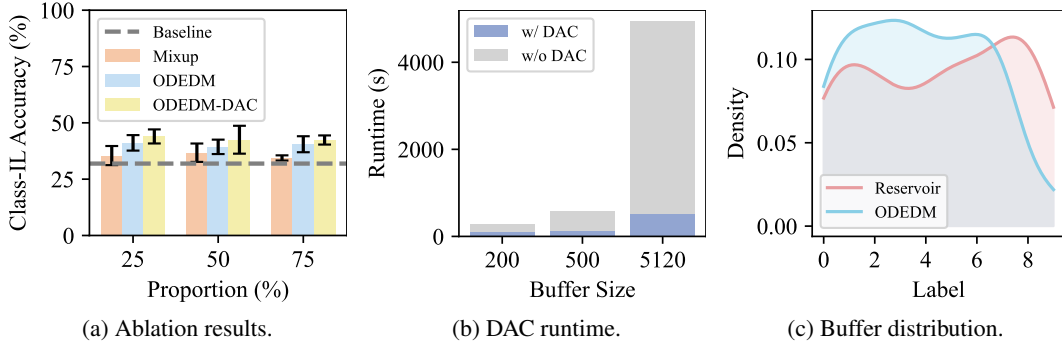


Figure 3: (a) The ablation study of the proposed ODEDM with Mixup, DAC and without DAC. (b) The runtime difference between with DAC and without DAC. (c) The buffer distribution of the proposed ODEDM with DAC on CIFAR10 under the imbalanced setting.

imbalance versus 28.7% without ODEDM (a 12 pp improvement). On CIFAR100 with a buffer of 500, the model-enabled DER++ matches or exceeds the vanilla best, scoring 10.2% compared to 8.4%. Even for TINYIMG, where imbalance inflicts the steepest declines, our approach consistently outperforms its non-augmented counterparts, demonstrating robustness to skewed data streams.

Forgetting curve. In order to investigate the effectiveness of our methods in mitigating catastrophic forgetting over multiple tasks, we consider performing the forgetting curve analysis. Specifically, we train various models with and without ODEDM on CIFAR10 under standard settings, while the maximum memory size is 200. Once each task switches, we calculate the classification error on all previously seen tasks, and the results are presented in Figure 2. From the empirical results, we can observe that the proposed ODEDM achieve significantly lower forgetting across all tasks compared to the other baselines. Such a result indicates that the proposed approach can preserve more critical data samples, which can encourage the model to combat network forgetting.

Short- and long-term memory. To investigate the dynamic process between the short-term and long-term memory buffers during the training process. Specifically, we train the proposed ODEDM on the CIFAR10, the CIFAR100 and the TINYIMG using three different memory configurations and the results are provided in Tables 4 to 6 from the SM in Appendix-B. From the empirical results, we can have several observations : (1) For the CIFAR10 and TINYIMG, using a large capacity for the long-term memory buffer can achieve a good performance; (2) The proposed ODEDM achieve different classification results when using the similar proportion of the short- and long-term memory buffers; (3) When considering a large memory capacity (the maximum number of memorised samples is 5120), changing the proportion of the short- and long-term memory buffer does not influence the model’s performance significantly.

Buffer distribution. To investigate the memory optimisation process, we train the proposed approach on the CIFAR10 with 75% of the long-term memory size, using DER++. We record the number of samples per category stored in the memory buffer after the whole training procedure is finished. We employ the Kernel Density Estimation (KDE) to estimate the probability density function of a random variable, to map the distribution in Figure 3c for the imbalanced setting. Figure 3c shows that the proposed approach can maintain balanced samples across previous tasks while reducing the number of samples in the final tasks. This makes the long-term memory in the proposed approach effectively preserve essential knowledge for previously encountered classes and ensure balanced memorised samples. In addition, Figure 3c indicates the reservoir sampling strategy, which is the most popular and standard sample selection approach in CL, forms a multimodal distribution, further validating the robustness of the proposed approach under the OCBBL setting.

4.3 Ablation Study

The DAC configuration. As depicted in Figure 3a, we can observe that the proposed ODEDM with DAC achieves the best performance. The vanilla dynamic dual buffer method (Mixup) achieves slightly better performance than the baseline method (DER++refresh). This indicates that the proposed ODEDM with DAC not only improves the performance of ODEDM but also significantly speeds up the training process, as shown in Figure 3b, measured by a NVIDIA GeForce RTX 3090.

The distance metric analysis. To analyse the distribution of long-term memory samples in the CIFAR10 feature space, we apply PCA [20] for visualisation. Then, we learn a linear mapping from the long-term memory buffer to full dataset embeddings via ordinary least squares and compute their cosine similarity to quantitatively evaluate how well each distance metric preserves the underlying data manifold,. In Figure 4 from the SM in Appendix-B, L2 and Sinkhorn achieve the highest alignment. Sample selections for each metric are visualised in Figures 5 to 8 from the SM in Appendix-B. Although all four distance-based selection metrics yield comparable average cosine similarities, their impact on performance differs. Under the DER++refresh with ODEDM, the L1 criterion attains a Class-IL accuracy of 41.09%, the L2 criterion achieves 44.00%, the MMD criterion reaches 36.93%, and the Sinkhorn criterion obtains 45.01%. These results suggest that, even when similarity scores are closely clustered, the choice of distance metric can meaningfully influence the effectiveness of memory-buffered rehearsal.

5 Conclusion and Limitations

This paper addresses a challenging online continual learning (CL) by proposing a novel dynamic memory allocation: Online Dynamic Expandable Dual Memory (ODEDM), which manages a short- and long-term memory buffer to preserve critical past samples. A novel memory optimisation approach is proposed to store critical samples in the long-term memory buffer selectively. Additionally, a Divide-and-Conquer (DAC) strategy is introduced to accelerate memory allocation. Experiments show that rehearsal-based models consistently perform better with ODEDM than without it. The primary limitation of ODEDM is that the proposed approach is only applied to supervised learning. In our future study, we will explore the proposed approach to unsupervised CL.

References

- [1] Ari S. Benjamin, David Rolnick, and Konrad Kording. Measuring and regularizing networks in function space, 2019.
- [2] Matteo Boschini, Lorenzo Bonicelli, Pietro Buzzega, Angelo Porrello, and Simone Calderara. Class-incremental continual learning into the extended der-verse. *IEEE Transactions on Pattern Analysis and Machine Intelligence*, 2022.
- [3] Bernhard E. Boser, Isabelle M. Guyon, and Vladimir N. Vapnik. A training algorithm for optimal margin classifiers. In *Proceedings of the Fifth Annual Workshop on Computational Learning Theory*, COLT '92, page 144–152, New York, NY, USA, 1992. Association for Computing Machinery.
- [4] Pietro Buzzega, Matteo Boschini, Angelo Porrello, Davide Abati, and Simone Calderara. Dark experience for general continual learning: a strong, simple baseline, 2020.
- [5] Pietro Buzzega, Matteo Boschini, Angelo Porrello, Davide Abati, and Simone Calderara. Dark experience for general continual learning: a strong, simple baseline. In H. Larochelle, M. Ranzato, R. Hadsell, M. F. Balcan, and H. Lin, editors, *Advances in Neural Information Processing Systems*, volume 33, pages 15920–15930. Curran Associates, Inc., 2020.
- [6] Francisco M. Castro, Manuel J. Marín-Jiménez, Nicolás Guil, Cordelia Schmid, and Karteek Alahari. End-to-end incremental learning, 2018.
- [7] Arslan Chaudhry, Marcus Rohrbach, Mohamed Elhoseiny, Thalaiyasingam Ajanthan, Puneet K. Dokania, Philip H. S. Torr, and Marc’Aurelio Ranzato. On tiny episodic memories in continual learning, 2019.
- [8] Marco Cuturi. Sinkhorn distances: Lightspeed computation of optimal transport. *Advances in neural information processing systems*, 26, 2013.
- [9] Marco Cuturi. Sinkhorn distances: Lightspeed computation of optimal transportation distances, 2013.
- [10] Matthias Delange, Rahaf Aljundi, Marc Masana, Sarah Parisot, Xu Jia, Ales Leonardis, Greg Slabaugh, and Tinne Tuytelaars. A continual learning survey: Defying forgetting in classification tasks. *IEEE Transactions on Pattern Analysis and Machine Intelligence*, page 1–1, 2021.
- [11] Prithviraj Dhar, Rajat Vikram Singh, Kuan-Chuan Peng, Ziyuan Wu, and Rama Chellappa. Learning without memorizing, 2019.
- [12] Arthur Douillard, Matthieu Cord, Charles Ollion, Thomas Robert, and Eduardo Valle. Podnet: Pooled outputs distillation for small-tasks incremental learning, 2020.

- [13] Jianping Gou, Baosheng Yu, Stephen J. Maybank, and Dacheng Tao. Knowledge distillation: A survey. *International Journal of Computer Vision*, 129(6):1789–1819, March 2021.
- [14] Arthur Gretton, Karsten M. Borgwardt, Malte J. Rasch, Bernhard Schölkopf, and Alexander J. Smola. A kernel method for the two-sample problem. *CoRR*, abs/0805.2368, 2008.
- [15] K. He, X. Zhang, S. Ren, and J. Sun. Deep residual learning for image recognition. In *Proc. of IEEE Conf. on Computer Vision and Pattern Recognition (CVPR)*, pages 770–778, 2016.
- [16] Kaiming He, Xiangyu Zhang, Shaoqing Ren, and Jian Sun. Deep residual learning for image recognition, 2015.
- [17] Saihui Hou, Xinyu Pan, Chen Change Loy, Zilei Wang, and Dahua Lin. Learning a unified classifier incrementally via rebalancing. *2019 IEEE/CVF Conference on Computer Vision and Pattern Recognition (CVPR)*, pages 831–839, 2019.
- [18] Steven C. Y. Hung, Cheng-Hao Tu, Cheng-En Wu, Chien-Hung Chen, Yi-Ming Chan, and Chu-Song Chen. Compacting, picking and growing for unforgetting continual learning, 2019.
- [19] Ahmet Iscen, Jeffrey Zhang, Svetlana Lazebnik, and Cordelia Schmid. Memory-efficient incremental learning through feature adaptation, 2020.
- [20] Ian T Jolliffe. *Principal component analysis for special types of data*. Springer, 2002.
- [21] Haeyong Kang, Jaehong Yoon, Sultan Rizky Madjid, Sung Ju Hwang, and Chang D. Yoo. Forget-free continual learning with soft-winning subnetworks, 2023.
- [22] James Kirkpatrick, Razvan Pascanu, Neil Rabinowitz, Joel Veness, Guillaume Desjardins, Andrei A. Rusu, Kieran Milan, John Quan, Tiago Ramalho, Agnieszka Grabska-Barwinska, Demis Hassabis, Claudia Clopath, Dharshan Kumaran, and Raia Hadsell. Overcoming catastrophic forgetting in neural networks. *Proceedings of the National Academy of Sciences*, 114(13):3521–3526, March 2017.
- [23] Alex Krizhevsky. Learning multiple layers of features from tiny images. 2009.
- [24] Alex Krizhevsky, Vinod Nair, and Geoffrey Hinton. Cifar-100 (canadian institute for advanced research).
- [25] S. Kullback and R. A. Leibler. On Information and Sufficiency. *The Annals of Mathematical Statistics*, 22(1):79 – 86, 1951.
- [26] Zhizhong Li and Derek Hoiem. Learning without forgetting. *IEEE Transactions on Pattern Analysis and Machine Intelligence*, 40:2935–2947, 2016.
- [27] Xialei Liu, Chenshen Wu, Mikel Menta, Luis Herranz, Bogdan Raducanu, Andrew D. Bagdanov, Shangling Jui, and Joost van de Weijer. Generative feature replay for class-incremental learning, 2020.
- [28] J MacQueen. Some methods for classification and analysis of multivariate observations. In *Proceedings of 5-th Berkeley Symposium on Mathematical Statistics and Probability/University of California Press*, 1967.
- [29] Arun Mallya, Dillon Davis, and Svetlana Lazebnik. Piggyback: Adapting a single network to multiple tasks by learning to mask weights, 2018.
- [30] James L McClelland, Bruce L McNaughton, and Randall C O'Reilly. Why there are complementary learning systems in the hippocampus and neocortex: insights from the successes and failures of connectionist models of learning and memory. *Psychological review*, 102(3):419, 1995.
- [31] G. I. Parisi, R. Kemker, J. L. Part, C. Kanan, and S. Wermter. Continual lifelong learning with neural networks: A review. *Neural Networks*, 113:54–71, 2019.
- [32] Sylvestre-Alvise Rebuffi, Alexander Kolesnikov, Georg Sperl, and Christoph H. Lampert. icarl: Incremental classifier and representation learning, 2017.
- [33] Matthew Riemer, Ignacio Cases, Robert Ajemian, Miao Liu, Irina Rish, Yuhai Tu, and Gerald Tesauro. Learning to learn without forgetting by maximizing transfer and minimizing interference, 2019.
- [34] Herbert Robbins and Sutton Monro. A stochastic approximation method. *The annals of mathematical statistics*, pages 400–407, 1951.
- [35] Jian Shen, Yanru Qu, Weinan Zhang, and Yong Yu. Wasserstein distance guided representation learning for domain adaptation, 2018.

- [36] Hanul Shin, Jung Kwon Lee, Jaehong Kim, and Jiwon Kim. Continual learning with deep generative replay, 2017.
- [37] Cédric Villani. *The Wasserstein distances*, pages 93–111. 01 2009.
- [38] Jeffrey S. Vitter. Random sampling with a reservoir. *ACM Trans. Math. Softw.*, 11(1):37–57, mar 1985.
- [39] Liyuan Wang, Xingxing Zhang, Hang Su, and Jun Zhu. A comprehensive survey of continual learning: Theory, method and application. *IEEE Transactions on Pattern Analysis and Machine Intelligence*, 46(8):5362–5383, 2024.
- [40] Zhenyi Wang, Yan Li, Li Shen, and Heng Huang. A unified and general framework for continual learning, 2024.
- [41] Mitchell Wortsman, Vivek Ramanujan, Rosanne Liu, Aniruddha Kembhavi, Mohammad Rastegari, Jason Yosinski, and Ali Farhadi. Supermasks in superposition, 2020.
- [42] Chenshen Wu, Luis Herranz, Xialei Liu, Yaxing Wang, Joost van de Weijer, and Bogdan Raducanu. Memory replay gans: learning to generate images from new categories without forgetting, 2019.
- [43] Jiayu Wu, Qixiang Zhang, and Guoxi Xu. Tiny imagenet challenge. 2017.
- [44] Jaehong Yoon, Eunho Yang, Jeongtae Lee, and Sung Ju Hwang. Lifelong learning with dynamically expandable networks, 2018.
- [45] Friedemann Zenke, Ben Poole, and Surya Ganguli. Continual learning through synaptic intelligence, 2017.
- [46] Mengyao Zhai, Lei Chen, Fred Tung, Jiawei He, Megha Nawhal, and Greg Mori. Lifelong gan: Continual learning for conditional image generation, 2019.
- [47] Kai Zhu, Wei Zhai, Yang Cao, Jiebo Luo, and Zheng-Jun Zha. Self-sustaining representation expansion for non-exemplar class-incremental learning, 2022.

A Algorithm Details

Algorithm 1: The training of ODEDM

Input: The total number of tasks n ;
 The proportion ρ of $\mathcal{M}_i^{\text{long}}$;
 The model's initial parameters;
Output: The model's updated parameters;
for $i = 1$ **to** n **do**

Step 1 (Find the cluster prototype).:
if $i \geq 1$ **then**
 $k_i = F_k(\rho)$;
 $\mathbf{C}_i = F_c(D_j)$;
foreach $c_j \in \mathbf{C}_i$ **do**
 $D_i(c_j) = F_{\text{class}}(D_i, c_j)$;
 Use the Divide-and-Conquer method;
 $\{\mathbf{x}_1^{c_j}, \dots, \mathbf{x}_k^{c_j}\} = F_{\text{centre}}(D_i(c_j), k)$;
Step 2 (Accumulate the data samples).:
for $h = 1$ **to** k **do**
 Obtain $\mathcal{M}(c_j, h)$ using the sample selection criterion;

Step 3 (The model update).:
for $j' = 1$ **to** n' **do**
 Obtain the new data batch $\mathbf{X}_{j'}$ from D_i ;
 Update the model on $\mathbf{X}_{j'}$ and selected samples;

Algorithm 2: Divide-and-Conquer

Input: Point set \mathcal{X} ; number of clusters k ;
 minimum merge size m ; recursion depth d ;
Output: Final cluster \mathcal{X}^* and its cardinality;
if $k = 0$ **or** $d = 0$ **then**
 $\quad \text{return } \mathcal{X}, |\mathcal{X}|$;

Step 1 (Initial partition).:
 Compute k clusters with K -Means:
 $\{\mathcal{C}_1, \dots, \mathcal{C}_k\} \leftarrow K\text{-Means}(\mathcal{X}, k)$

Step 2 (Build point clouds).:
for $i = 1 \dots k$ **do**
 $\quad \mathcal{P}_i \leftarrow \mathcal{C}_i$

Step 3 (Pairwise distances).:
 Initialise $D \in \mathbb{R}^{k \times k}$ to ∞ ;
for $1 \leq i < j \leq k$ **do**
 $\quad \text{Compute uniform weights } w_i, w_j \text{ for } \mathcal{P}_i, \mathcal{P}_j$;
 $\quad D_{i,j} = D_{j,i} \leftarrow \text{Sinkhorn}(\mathcal{P}_i, \mathcal{P}_j, w_i, w_j)$;

Step 4 (Select merge path).:
 Let $\mathcal{S} = \{1, \dots, k\}$ and $(\pi^*, \delta^*, N^*) \leftarrow \text{find_best_path}(D, \{|\mathcal{P}_i|\}, m)$ **if** $\pi^* = \emptyset$
then
 $\quad \text{return } \mathcal{X}, |\mathcal{X}|$;

Step 5 (Merge and recurse).:
 $\mathcal{M} \leftarrow \bigcup_{i \in \pi^*} \mathcal{P}_i$;
return Divide-and-conquer($\mathcal{M}, k, m, d - 1$);

B Additional Experimental Results

Table 2: Approximation of k across various datasets. " k (%)" denotes the number of k values used in ODEDM and represents the proportion of long-term memory relative to the total buffer size. We can calculate the proportion using $|M_n^{\text{long}}| + (n-1) \times k \times |c_j| \simeq \lceil |M_n| \times \rho \rceil$, where n is the task number, and c_j denotes the number of classes in a given task.

Buffer Size	CIFAR10	CIFAR100	TINYIMG
200	6 (24%)	-	-
	13 (52%)	1 (45%)	-
	19 (76%)	-	1 (90%)
500	16 (26%)	1 (18%)	1 (36%)
	31 (50%)	3 (54%)	-
	47 (75%)	4 (72%)	2 (72%)
5120	160 (25%)	14 (25%)	7 (25%)
	320 (50%)	28 (49%)	14 (49%)
	480 (75%)	42 (74%)	21 (74%)

Table 3: Performance of DER++refresh on CIFAR-10 under varying class proportions, number of clusters (K), and depth in DAC, with a buffer size of 200. The best-performing configuration for each class proportion is highlighted in blue. For the 25% proportion, although the Class-IL performance for the configuration with $K = 3$ and depth 4 is comparable to that of $K = 4$ and depth 2, we select $K = 3$ and depth 4 as the optimal configuration due to its superior performance in Task-IL.

Proportion	K	depth	Class-IL	Task-IL
25%	3	2	43.37 \pm 1.81	81.86 \pm 3.06
	3	3	40.38 \pm 3.16	81.25 \pm 2.26
	3	4	43.81 \pm 2.25	82.50 \pm 3.72
	4	2	43.96 \pm 3.12	81.17 \pm 3.64
	4	3	38.75 \pm 3.52	78.70 \pm 2.76
	4	4	37.16 \pm 2.67	81.75 \pm 5.73
	5	2	40.55 \pm 4.39	79.40 \pm 3.89
	5	3	43.90 \pm 4.94	82.19 \pm 1.70
	5	4	40.95 \pm 1.91	84.87 \pm 1.23
	3	2	42.50 \pm 6.19	79.38 \pm 2.42
50%	3	2	42.50 \pm 6.19	79.38 \pm 2.42
	3	3	40.38 \pm 4.90	83.65 \pm 1.35
	3	4	40.30 \pm 1.00	81.58 \pm 0.79
	4	2	34.52 \pm 8.06	82.12 \pm 4.40
	4	3	37.86 \pm 1.01	81.22 \pm 1.84
	4	4	39.39 \pm 2.63	81.79 \pm 3.12
	5	2	34.27 \pm 7.25	80.09 \pm 2.41
	5	3	36.61 \pm 8.25	81.67 \pm 2.23
	5	4	35.26 \pm 4.57	77.95 \pm 5.66
	3	2	38.82 \pm 4.38	81.28 \pm 0.83
75%	3	3	40.12 \pm 0.75	79.53 \pm 2.40
	3	4	36.89 \pm 2.46	83.45 \pm 1.21
	4	2	37.01 \pm 1.89	77.79 \pm 0.72
	4	3	36.20 \pm 1.75	82.63 \pm 1.54
	4	4	37.40 \pm 3.32	80.97 \pm 1.30
	5	2	38.54 \pm 6.16	81.40 \pm 2.82
	5	3	42.38 \pm 2.03	78.69 \pm 1.93
	5	4	35.39 \pm 0.65	82.21 \pm 0.83

Table 4: Average accuracy (%) of ODEDM on CIFAR10 across three runs under standard and imbalanced settings with varying buffer sizes. The best results for each setting are indicated in **bold**.

Buffer Method	Standard		Imbalanced		
	Class-IL	Task-IL	Class-IL	Task-IL	
200	DER (ODEDM-6)	29.99 \pm 03.48	69.61 \pm 01.76	14.72 \pm 03.84	57.80 \pm 07.82
	DER (ODEDM-13)	26.93 \pm 03.10	75.25 \pm 02.30	22.04 \pm 05.85	67.07 \pm 06.62
	DER (ODEDM-19)	22.40 \pm 01.12	73.10 \pm 03.21	13.45 \pm 05.02	59.28 \pm 07.96
	DER++ (ODEDM-6)	42.69 \pm 01.51	81.34 \pm 01.61	40.95 \pm 01.82	82.27 \pm 01.65
	DER++ (ODEDM-13)	42.71 \pm 01.86	79.53 \pm 04.29	35.03 \pm 07.70	78.62 \pm 02.77
	DER++ (ODEDM-19)	38.69 \pm 00.69	78.35 \pm 02.17	31.81 \pm 01.83	76.22 \pm 03.25
	DER++refresh (ODEDM-6)	41.63 \pm 01.75	80.49 \pm 03.95	37.56 \pm 03.08	77.69 \pm 02.72
	DER++refresh (ODEDM-13)	42.47 \pm 00.38	85.56 \pm 00.74	38.41 \pm 00.88	79.79 \pm 00.75
	DER++refresh (ODEDM-19)	36.19 \pm 04.73	82.68 \pm 01.14	35.88 \pm 01.67	79.20 \pm 01.11
	FDR (ODEDM-6)	21.15 \pm 05.54	67.12 \pm 06.33	21.14 \pm 01.72	68.20 \pm 03.27
	FDR (ODEDM-13)	17.56 \pm 02.85	66.31 \pm 04.40	20.18 \pm 02.53	63.77 \pm 02.12
	FDR (ODEDM-19)	25.17 \pm 01.39	73.76 \pm 05.98	16.88 \pm 02.15	63.70 \pm 06.24
500	iCaRL (ODEDM-6)	37.64 \pm 01.56	89.88 \pm 01.72	35.26 \pm 00.58	81.94 \pm 05.76
	iCaRL (ODEDM-13)	36.65 \pm 02.96	85.40 \pm 03.42	32.21 \pm 02.71	80.78 \pm 05.69
	iCaRL (ODEDM-19)	31.42 \pm 02.32	83.45 \pm 02.96	29.93 \pm 01.34	81.57 \pm 04.09
	DER (ODEDM-16)	24.98 \pm 05.26	75.26 \pm 05.04	20.37 \pm 05.56	61.48 \pm 04.06
	DER (ODEDM-31)	28.34 \pm 04.98	70.96 \pm 03.70	19.60 \pm 02.65	70.92 \pm 03.97
	DER (ODEDM-47)	23.18 \pm 03.64	72.68 \pm 05.20	21.32 \pm 05.02	62.80 \pm 06.85
	DER++ (ODEDM-16)	47.31 \pm 02.62	83.46 \pm 01.02	40.14 \pm 02.46	82.85 \pm 00.65
	DER++ (ODEDM-31)	45.53 \pm 03.39	83.05 \pm 01.19	39.51 \pm 04.05	76.59 \pm 02.68
	DER++ (ODEDM-47)	44.67 \pm 01.08	83.37 \pm 00.19	36.69 \pm 03.99	75.66 \pm 01.49
	DER++refresh (ODEDM-16)	46.17 \pm 02.37	84.77 \pm 02.58	29.11 \pm 10.39	72.08 \pm 02.30
	DER++refresh (ODEDM-31)	38.30 \pm 11.61	81.19 \pm 04.23	41.53 \pm 04.15	77.49 \pm 05.68
	DER++refresh (ODEDM-47)	44.21 \pm 00.61	83.14 \pm 01.60	40.38 \pm 01.94	79.47 \pm 03.30
5120	FDR (ODEDM-16)	24.43 \pm 01.04	77.52 \pm 02.14	16.59 \pm 01.16	67.96 \pm 02.47
	FDR (ODEDM-31)	19.52 \pm 02.91	68.20 \pm 01.74	16.75 \pm 01.59	65.12 \pm 04.38
	FDR (ODEDM-47)	15.78 \pm 01.37	64.49 \pm 06.19	17.50 \pm 01.57	59.64 \pm 02.36
	iCaRL (ODEDM-16)	35.42 \pm 04.39	80.84 \pm 07.76	35.56 \pm 02.25	85.26 \pm 02.64
	iCaRL (ODEDM-31)	38.31 \pm 00.72	86.81 \pm 03.38	34.70 \pm 01.56	80.89 \pm 01.93
	iCaRL (ODEDM-47)	35.04 \pm 02.75	86.61 \pm 02.97	36.10 \pm 00.87	85.30 \pm 02.96
	DER (ODEDM-160)	21.81 \pm 04.02	66.60 \pm 03.06	18.94 \pm 05.34	58.35 \pm 03.24
	DER (ODEDM-320)	29.96 \pm 01.63	66.24 \pm 02.21	21.89 \pm 04.60	63.16 \pm 02.46
	DER (ODEDM-480)	26.34 \pm 03.87	76.19 \pm 03.84	17.91 \pm 00.73	65.31 \pm 01.93
	DER++ (ODEDM-160)	54.49 \pm 01.44	87.77 \pm 03.28	43.37 \pm 03.58	81.29 \pm 04.82
	DER++ (ODEDM-320)	49.81 \pm 09.49	85.95 \pm 03.53	44.34 \pm 05.27	86.64 \pm 01.70
	DER++ (ODEDM-480)	48.75 \pm 10.79	84.18 \pm 08.06	47.90 \pm 02.10	87.37 \pm 02.42
5120	DER++refresh (ODEDM-160)	55.14 \pm 02.30	87.82 \pm 01.57	45.22 \pm 04.63	84.50 \pm 04.13
	DER++refresh (ODEDM-320)	55.17 \pm 02.30	90.32 \pm 03.62	43.68 \pm 01.83	77.80 \pm 01.75
	DER++refresh (ODEDM-480)	52.87 \pm 01.06	87.70 \pm 01.89	42.39 \pm 00.88	81.12 \pm 03.78
	FDR (ODEDM-160)	16.84 \pm 00.75	64.69 \pm 06.23	17.26 \pm 01.35	69.99 \pm 03.47
	FDR (ODEDM-320)	18.33 \pm 00.58	64.53 \pm 04.79	17.86 \pm 00.14	61.47 \pm 03.36
	FDR (ODEDM-480)	17.48 \pm 00.78	67.21 \pm 05.14	16.00 \pm 00.00	63.00 \pm 00.00
5120	iCaRL (ODEDM-160)	47.50 \pm 00.88	90.27 \pm 01.56	44.78 \pm 02.11	85.40 \pm 01.81
	iCaRL (ODEDM-320)	44.43 \pm 01.20	88.27 \pm 01.63	38.94 \pm 02.82	87.87 \pm 01.47
	iCaRL (ODEDM-480)	43.72 \pm 01.43	84.29 \pm 02.60	41.79 \pm 01.91	84.39 \pm 02.71

Table 5: Average accuracy (%) of ODEDM on CIFAR100 across three runs under standard and imbalanced settings with varying buffer sizes. The best results for each setting are indicated in **bold**.

Buffer Method	Standard		Imbalanced		
	<i>Class-IL</i>	<i>Task-IL</i>	<i>Class-IL</i>	<i>Task-IL</i>	
200	DER (ODEDM-1)	04.78 \pm 00.56	25.53 \pm 02.25	03.20 \pm 00.71	20.77 \pm 02.63
	DER++ (ODEDM-1)	07.78 \pm 01.78	38.27 \pm 04.86	07.46 \pm 01.57	38.66 \pm 03.79
	DER++refresh (ODEDM-1)	08.47 \pm 01.24	41.17 \pm 00.87	05.68 \pm 01.99	34.87 \pm 05.62
	FDR (ODEDM-1)	04.14 \pm 00.52	23.10 \pm 03.18	03.49 \pm 00.55	21.11 \pm 03.55
	iCaRL (ODEDM-1)	01.03 \pm 00.02	07.05 \pm 01.19	01.17 \pm 00.34	06.28 \pm 01.33
	DER (ODEDM-1)	04.12 \pm 00.81	24.88 \pm 01.12	03.61 \pm 01.09	21.33 \pm 03.94
500	DER (ODEDM-3)	03.63 \pm 00.38	22.15 \pm 01.55	03.75 \pm 00.54	22.21 \pm 01.70
	DER (ODEDM-4)	04.10 \pm 00.89	22.31 \pm 03.58	03.84 \pm 00.34	23.59 \pm 01.54
	DER++ (ODEDM-1)	10.77 \pm 03.76	45.26 \pm 06.63	10.16 \pm 00.55	44.82 \pm 02.34
	DER++ (ODEDM-3)	13.62 \pm 02.51	50.26 \pm 02.38	08.16 \pm 00.99	43.40 \pm 01.46
	DER++ (ODEDM-4)	11.30 \pm 00.59	47.70 \pm 00.56	07.53 \pm 00.87	43.26 \pm 02.48
	DER++refresh (ODEDM-1)	09.11 \pm 03.63	44.83 \pm 04.61	10.27 \pm 01.19	45.69 \pm 02.42
5120	DER++refresh (ODEDM-3)	08.93 \pm 01.19	46.30 \pm 01.57	09.69 \pm 02.35	43.89 \pm 03.38
	DER++refresh (ODEDM-4)	11.79 \pm 01.91	47.21 \pm 00.63	08.26 \pm 03.15	42.65 \pm 04.40
	FDR (ODEDM-1)	04.73 \pm 00.81	25.51 \pm 02.24	03.96 \pm 00.45	25.18 \pm 01.66
	FDR (ODEDM-3)	04.90 \pm 00.40	29.50 \pm 02.47	04.09 \pm 00.69	22.23 \pm 04.34
	FDR (ODEDM-4)	04.96 \pm 00.84	28.67 \pm 01.96	04.71 \pm 00.66	25.86 \pm 01.47
	iCaRL (ODEDM-1)	07.35 \pm 00.14	33.70 \pm 00.45	07.49 \pm 00.40	32.81 \pm 01.27
	iCaRL (ODEDM-3)	00.95 \pm 00.08	08.75 \pm 00.66	00.99 \pm 00.19	09.29 \pm 00.69
	iCaRL (ODEDM-4)	01.07 \pm 00.18	08.28 \pm 00.96	01.17 \pm 00.12	08.91 \pm 00.68
	DER (ODEDM-14)	03.46 \pm 00.15	24.25 \pm 02.44	02.92 \pm 00.78	18.84 \pm 02.60
	DER (ODEDM-28)	04.83 \pm 00.33	26.29 \pm 01.48	02.73 \pm 00.48	20.76 \pm 02.96
	DER (ODEDM-42)	03.92 \pm 00.74	23.44 \pm 02.05	02.54 \pm 00.97	18.54 \pm 04.31
	DER++ (ODEDM-14)	22.42 \pm 05.67	61.76 \pm 05.09	11.53 \pm 02.53	50.53 \pm 07.10
	DER++ (ODEDM-28)	16.47 \pm 01.28	58.53 \pm 03.26	13.62 \pm 03.94	53.41 \pm 02.51
	DER++ (ODEDM-42)	15.04 \pm 03.61	57.57 \pm 03.07	12.38 \pm 05.90	53.39 \pm 01.38
	DER++refresh (ODEDM-14)	15.11 \pm 02.96	56.36 \pm 05.40	15.15 \pm 01.92	52.73 \pm 02.98
	DER++refresh (ODEDM-28)	21.60 \pm 03.27	63.24 \pm 00.85	11.84 \pm 04.73	54.34 \pm 01.98
	DER++refresh (ODEDM-42)	18.73 \pm 06.21	59.90 \pm 03.95	13.30 \pm 04.21	47.47 \pm 04.97
	FDR (ODEDM-14)	06.04 \pm 00.94	29.69 \pm 06.18	04.76 \pm 00.64	27.68 \pm 01.61
	FDR (ODEDM-28)	05.17 \pm 00.72	30.30 \pm 02.69	04.60 \pm 00.26	25.52 \pm 01.41
	FDR (ODEDM-42)	04.98 \pm 00.76	29.42 \pm 02.04	04.94 \pm 00.12	28.15 \pm 00.63
	iCaRL (ODEDM-14)	08.49 \pm 00.35	35.42 \pm 00.67	07.58 \pm 00.54	33.80 \pm 01.77
	iCaRL (ODEDM-28)	09.28 \pm 00.14	36.51 \pm 00.54	08.33 \pm 00.16	35.38 \pm 00.44
	iCaRL (ODEDM-42)	08.45 \pm 00.52	35.63 \pm 00.96	07.94 \pm 00.23	33.85 \pm 00.67

Table 6: Average accuracy (%) of ODEDM on TINYIMG across three runs under standard and imbalanced settings with varying buffer sizes. The best results for each setting are indicated in **bold**.

Buffer Method	Standard		Imbalanced		
	<i>Class-IL</i>	<i>Task-IL</i>	<i>Class-IL</i>	<i>Task-IL</i>	
200	DER (ODEDM-1)	03.83 \pm 00.27	17.21 \pm 00.29	02.82 \pm 00.45	14.44 \pm 01.40
	DER++ (ODEDM-1)	04.65 \pm 01.16	27.17 \pm 02.65	04.09 \pm 00.95	26.70 \pm 02.11
	DER++refresh (ODEDM-1)	05.25 \pm 01.09	28.04 \pm 00.88	03.29 \pm 00.73	23.28 \pm 03.68
	FDR (ODEDM-1)	04.18 \pm 00.31	18.65 \pm 03.00	03.51 \pm 00.50	15.70 \pm 02.60
	iCaRL (ODEDM-1)	—	—	—	—
500	DER (ODEDM-1)	04.45 \pm 00.12	20.52 \pm 01.00	03.55 \pm 00.17	18.28 \pm 00.57
	DER (ODEDM-2)	03.58 \pm 00.40	18.97 \pm 01.33	03.26 \pm 00.57	15.14 \pm 00.23
	DER++ (ODEDM-1)	07.43 \pm 00.75	34.96 \pm 04.37	05.56 \pm 00.64	31.60 \pm 01.65
	DER++ (ODEDM-2)	06.90 \pm 00.65	35.92 \pm 03.48	05.93 \pm 01.42	32.56 \pm 01.73
	DER++refresh (ODEDM-1)	07.14 \pm 00.85	35.66 \pm 01.90	07.00 \pm 00.79	33.13 \pm 01.75
5120	DER++refresh (ODEDM-2)	05.76 \pm 00.47	33.95 \pm 02.00	05.63 \pm 00.66	31.74 \pm 01.21
	FDR (ODEDM-1)	04.84 \pm 00.38	21.14 \pm 01.48	03.47 \pm 00.11	17.23 \pm 01.01
	FDR (ODEDM-2)	04.66 \pm 00.42	20.33 \pm 01.46	03.90 \pm 00.27	17.04 \pm 01.90
	iCaRL (ODEDM-1)	00.44 \pm 00.09	03.91 \pm 00.16	00.45 \pm 00.03	03.46 \pm 00.12
	iCaRL (ODEDM-2)	00.48 \pm 00.08	03.59 \pm 00.14	00.51 \pm 00.12	03.62 \pm 00.39
5120	DER (ODEDM-7)	04.37 \pm 00.49	20.62 \pm 00.84	03.27 \pm 00.36	17.35 \pm 00.86
	DER (ODEDM-14)	04.32 \pm 00.12	21.07 \pm 00.78	03.55 \pm 00.37	18.27 \pm 01.30
	DER (ODEDM-21)	04.49 \pm 00.48	20.28 \pm 00.52	03.22 \pm 00.27	16.13 \pm 00.36
	DER++ (ODEDM-7)	15.61 \pm 03.29	51.29 \pm 03.23	09.67 \pm 02.86	42.29 \pm 03.17
	DER++ (ODEDM-14)	13.38 \pm 01.09	48.58 \pm 02.44	11.13 \pm 01.72	45.89 \pm 03.28
5120	DER++ (ODEDM-21)	14.21 \pm 01.16	51.02 \pm 01.45	10.35 \pm 01.54	47.35 \pm 01.18
	DER++refresh (ODEDM-7)	15.88 \pm 01.37	53.08 \pm 00.80	12.71 \pm 01.17	47.61 \pm 02.07
	DER++refresh (ODEDM-14)	17.27 \pm 02.20	52.50 \pm 00.91	11.92 \pm 02.79	44.53 \pm 03.45
	DER++refresh (ODEDM-21)	17.65 \pm 00.43	53.27 \pm 02.02	10.83 \pm 01.01	45.85 \pm 01.39
	FDR (ODEDM-7)	04.79 \pm 00.39	22.22 \pm 02.69	04.22 \pm 00.33	21.09 \pm 01.93
5120	FDR (ODEDM-14)	04.77 \pm 00.66	21.82 \pm 00.36	04.53 \pm 00.12	20.66 \pm 00.26
	FDR (ODEDM-21)	05.01 \pm 00.23	23.18 \pm 02.81	04.69 \pm 00.22	20.94 \pm 01.30
	iCaRL (ODEDM-7)	03.97 \pm 00.14	19.25 \pm 00.49	03.85 \pm 00.18	18.23 \pm 00.47
	iCaRL (ODEDM-14)	04.01 \pm 00.02	19.10 \pm 00.19	03.68 \pm 00.08	17.88 \pm 00.22
	iCaRL (ODEDM-21)	03.81 \pm 00.11	18.39 \pm 00.64	03.37 \pm 00.20	17.45 \pm 00.49

Table 7: Average accuracy of DER++ across three runs with various buffer sizes on the ImageNet-R dataset. To assess performance on large-scale datasets, we report results under both standard and imbalanced settings to ensure a comprehensive evaluation. The best results in each setting are highlighted in **bold**.

Buffer Method	Standard		Imbalanced		
	<i>Class-IL</i>	<i>Task-IL</i>	<i>Class-IL</i>	<i>Task-IL</i>	
200	DER++refresh	00.94 \pm 00.37	08.34 \pm 00.55	00.87 \pm 00.28	06.62 \pm 00.43
	DER++refresh (ODEDM-1)	00.95 \pm 00.16	06.20 \pm 00.21	00.86 \pm 00.30	06.72 \pm 00.86
500	DER++refresh	00.75 \pm 00.24	08.70 \pm 00.62	00.75 \pm 00.05	08.24 \pm 00.10
	DER++refresh (ODEDM-1)	01.06 \pm 00.25	07.78 \pm 00.40	01.00 \pm 00.20	08.50 \pm 00.27
5120	DER++refresh (ODEDM-2)	00.82 \pm 00.30	07.59 \pm 00.86	00.93 \pm 00.20	06.99 \pm 00.70
	DER++refresh	00.78 \pm 00.13	10.11 \pm 00.50	00.64 \pm 00.04	08.53 \pm 00.22
	DER++refresh (ODEDM-7)	00.99 \pm 00.12	09.08 \pm 00.65	00.84 \pm 00.07	09.02 \pm 00.92
	DER++refresh (ODEDM-14)	01.14 \pm 00.11	09.07 \pm 00.58	00.75 \pm 00.31	09.79 \pm 01.08
5120	DER++refresh (ODEDM-21)	00.82 \pm 00.20	08.59 \pm 00.95	01.06 \pm 00.16	07.77 \pm 00.76

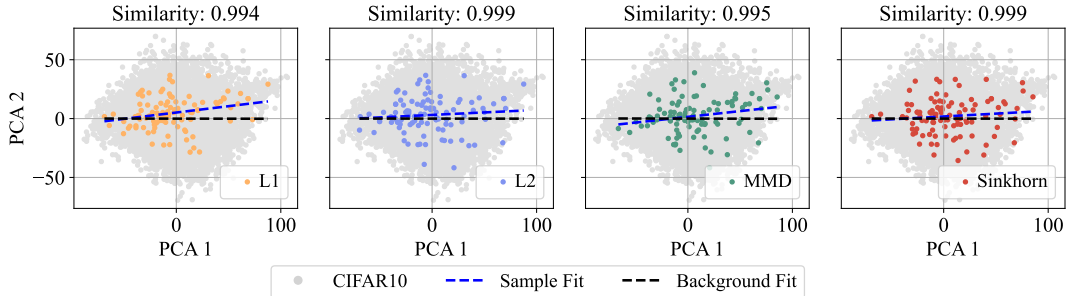


Figure 4: Visualisation of feature space in buffers and CIFAR10 with PCA under different distance metrics in ODEDM. We conduct an ablation study to compare the effects of various distance metrics, including L1, L2, Maximum Mean Discrepancy (MMD), and Sinkhorn, on DER++refresh with ODEDM trained on CIFAR10. Specifically, we select the first 1,000 samples from the CIFAR10 training set and all buffer samples retained by ODEDM under the 75% proportion for long-term buffers. These samples are first embedded into the feature space, after which PCA is applied to reduce the dimensionality to two dimensions. To quantify the alignment between the CIFAR10 and buffer distributions in feature space, we fit a linear mapping to each set of projected features and compute the cosine similarity between the resulting lines.

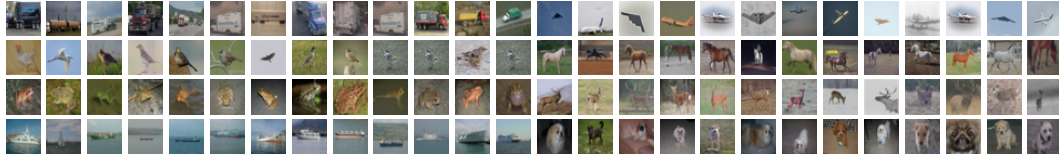


Figure 5: Samples selected using the L1 distance metric on CIFAR10, under the 75% long-term buffer proportion, with DER++refresh and ODEDM.

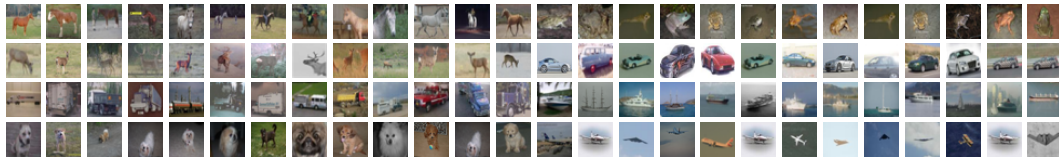


Figure 6: Samples selected using the L2 distance metric on CIFAR10, under the 75% long-term buffer proportion, with DER++refresh and ODEDM.

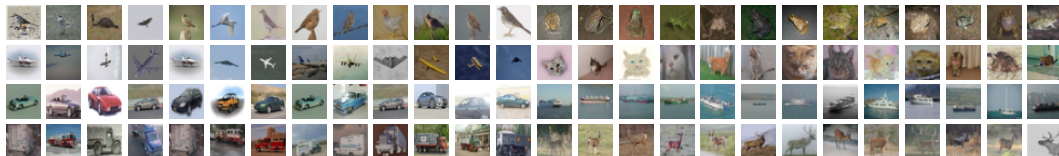


Figure 7: Samples selected using the MMD distance metric on CIFAR10, under the 75% long-term buffer proportion, with DER++refresh and ODEDM.

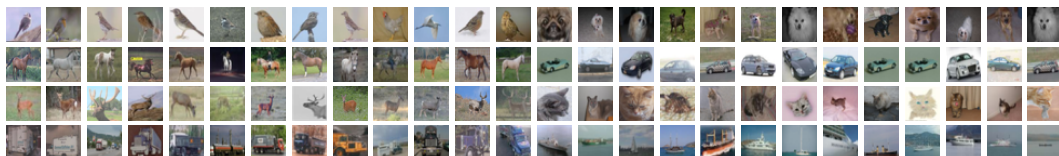


Figure 8: Samples selected using the Sinkhorn distance metric on CIFAR10, under the 75% long-term buffer proportion, with DER++refresh and ODEDM.